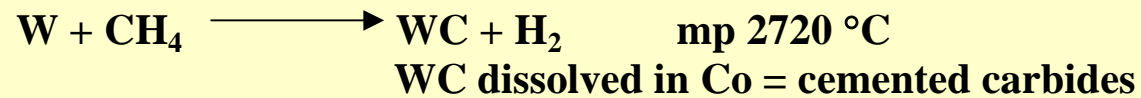
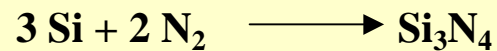
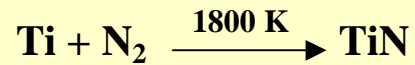


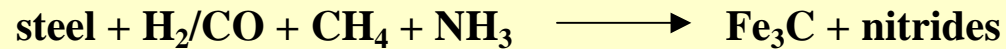
# Gas Phase Reactions

Heating: furnace, laser, plasma, flame, arc

## Gas-Metal Rxn



cementite



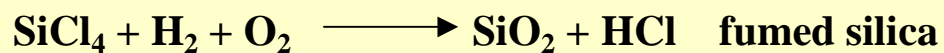
# Gas-Phase Reactions

## Gas-Gas Rxn

homogeneous nucleation from supersaturated vapor (nano)

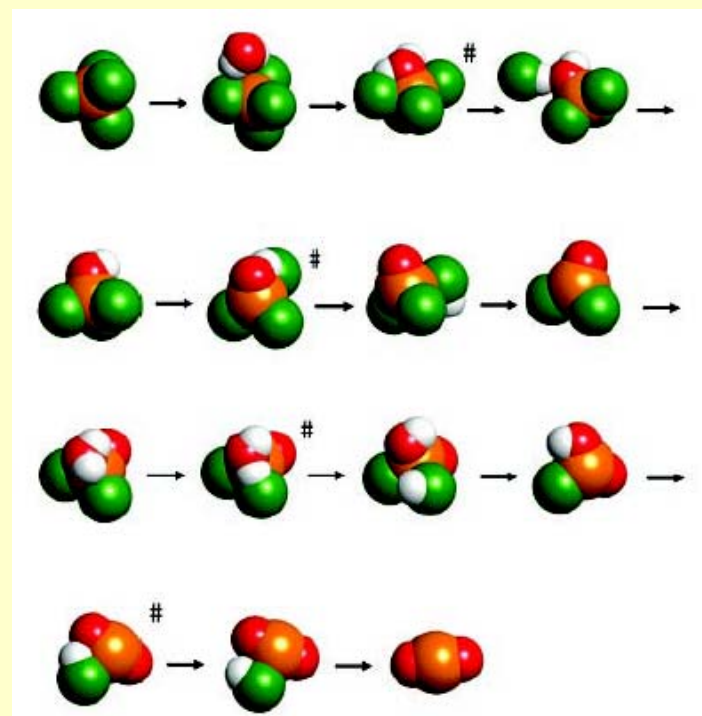
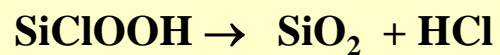
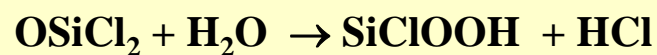
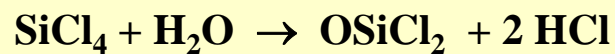
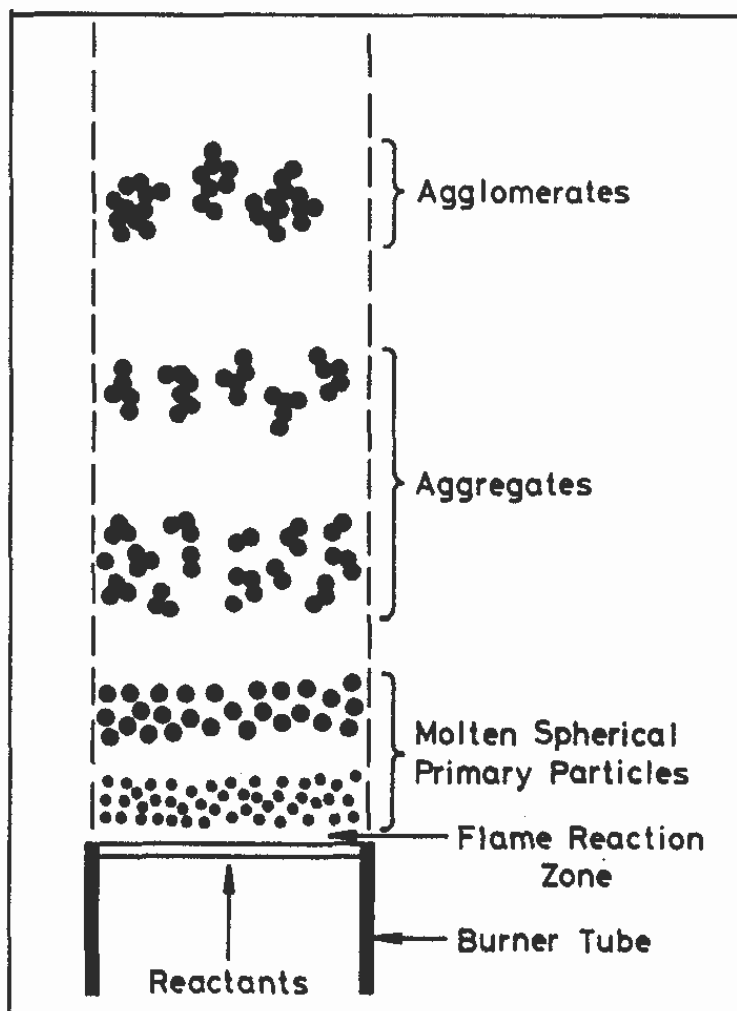
Flame hydrolysis

volatile compounds are passed through an oxygen-hydrogen stationary flame:

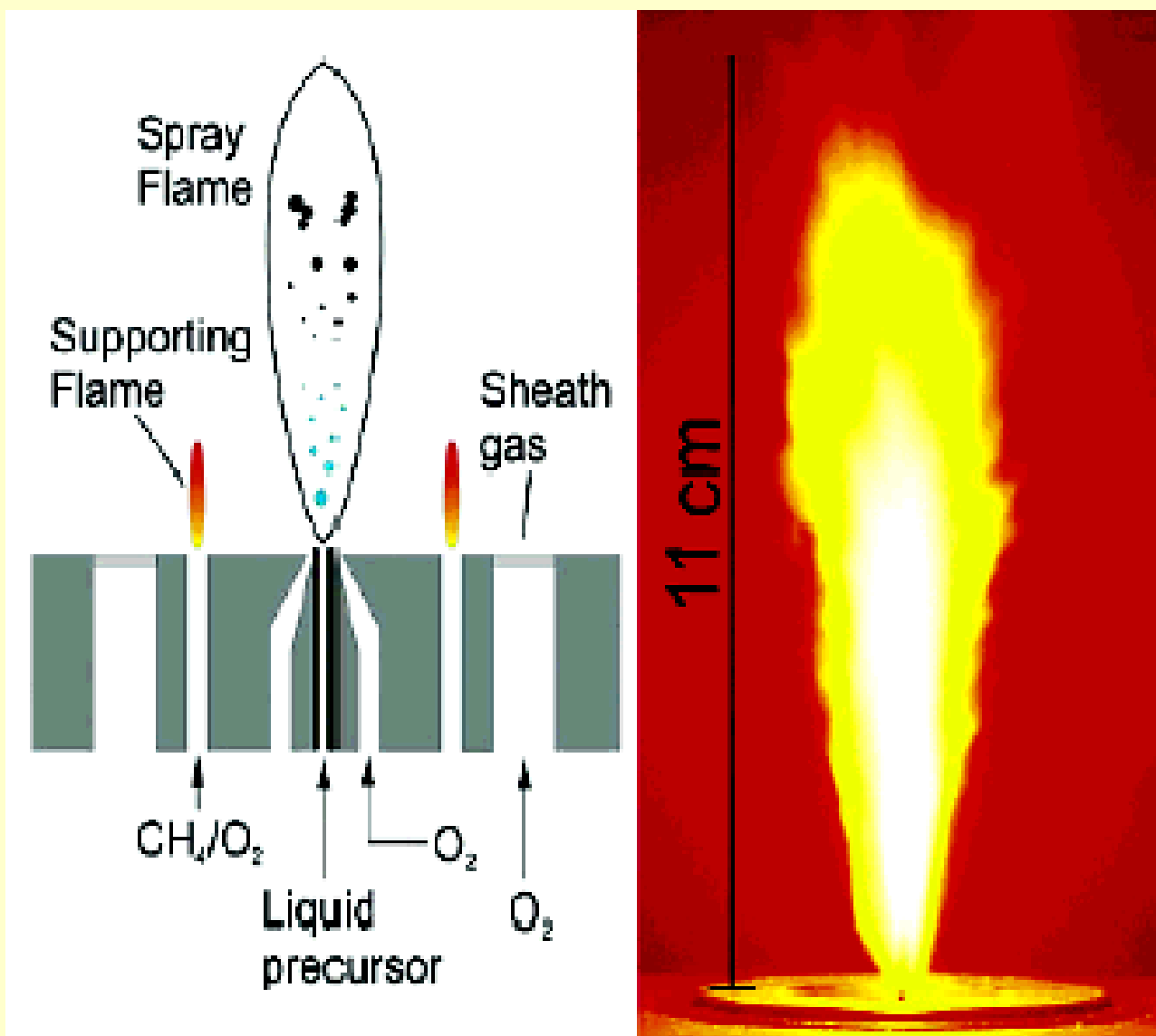


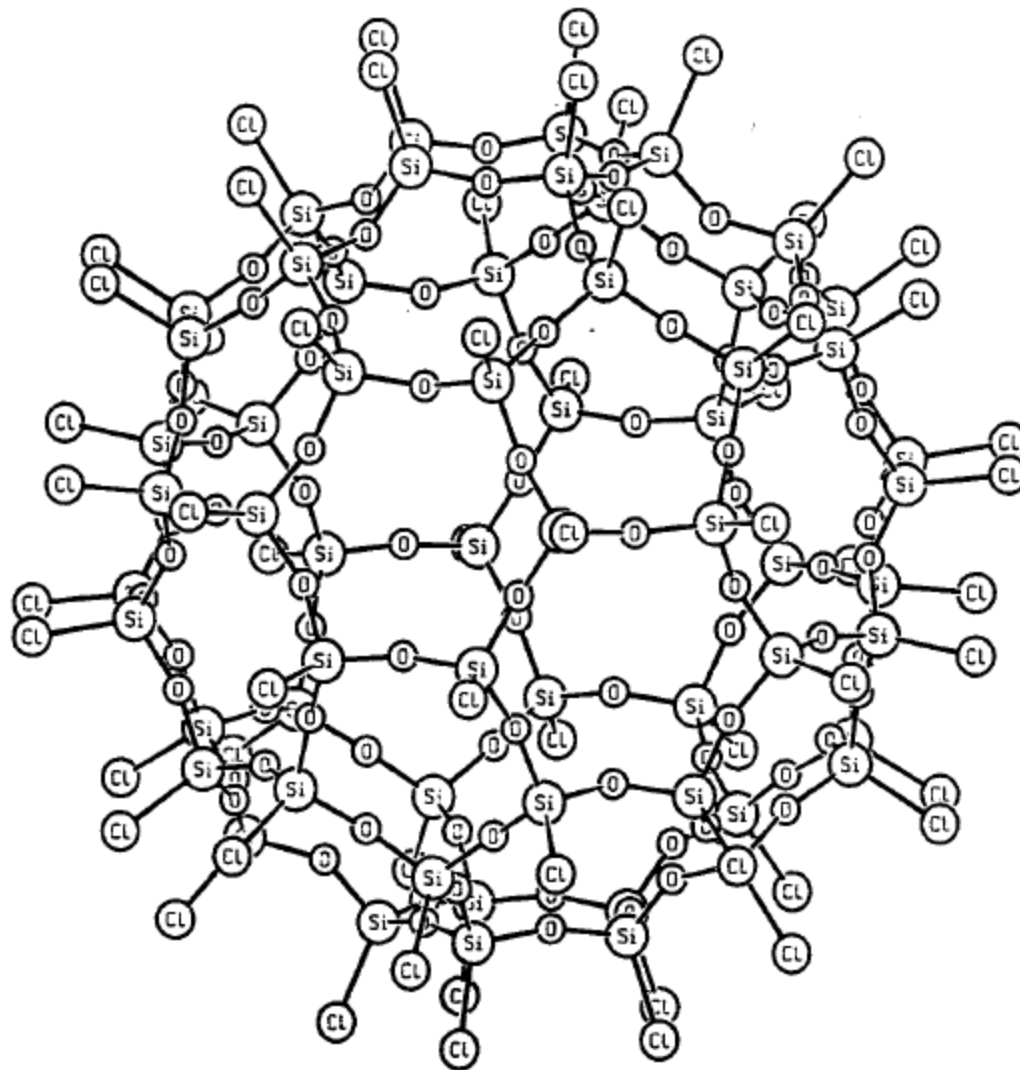
reagent	bp/°C	product
SiCl <sub>4</sub>	57	SiO <sub>2</sub>
AlCl <sub>3</sub>	180 (subl.)	Al <sub>2</sub> O <sub>3</sub>
TiCl <sub>4</sub>	137	TiO <sub>2</sub>
CrO <sub>2</sub> Cl <sub>2</sub>	117	Cr <sub>2</sub> O <sub>3</sub>
Fe(CO) <sub>5</sub>	103	Fe <sub>2</sub> O <sub>3</sub>
GeCl <sub>4</sub>	84	GeO <sub>2</sub>
Ni(CO) <sub>4</sub>	42	NiO
SnCl <sub>4</sub>	114	SnO <sub>2</sub>
ZrCl <sub>4</sub>	331 (subl.)	ZrO <sub>2</sub>
VOCl <sub>3</sub>	127	V <sub>2</sub> O <sub>5</sub>

# Gas Phase Reactions



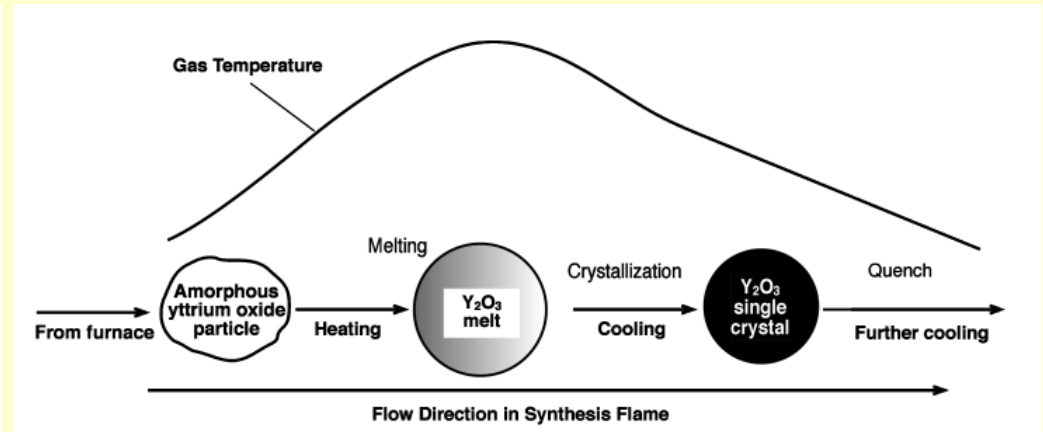
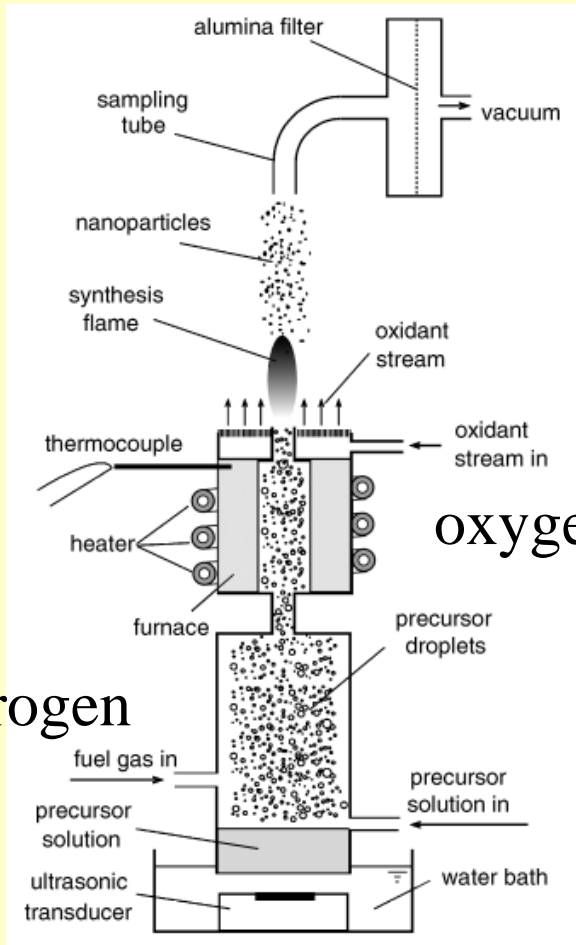
# Gas Phase Reactions





$\text{Si}_{60}\text{O}_{90}\text{Cl}_{60}$  ( $I_h$ )

# Y<sub>2</sub>O<sub>3</sub> Particles by Flame Aerosol Process



hydrogen

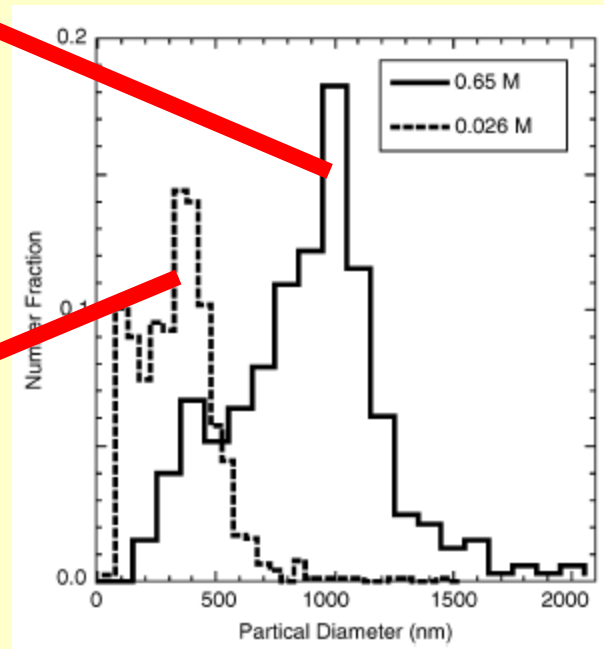
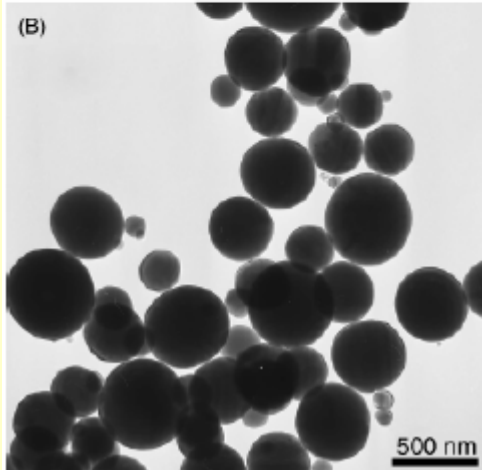
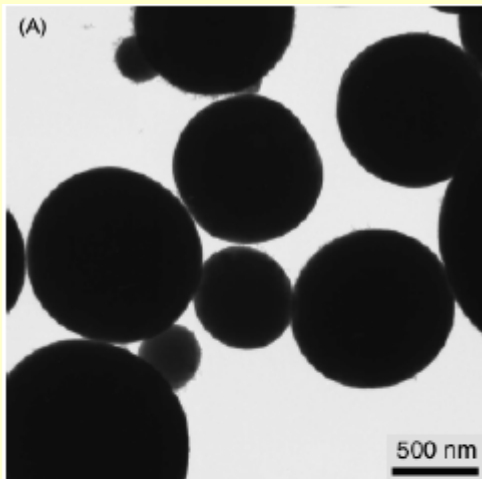
oxygen



# Particle Size Control

Particle size control by precursor concentration

Higher concentration = larger size



# Gas Phase Reactions

**Calcium phosphate nanoparticles Ca/P molar ratios 1.43 to 1.67**

**synthesized by simultaneous combustion of  
 $\text{Ca}(\text{OAc})_2 + \text{OP}(\text{O}^n\text{Bu})_3$  in a flame spray reactor**

**Fluoro-apatite and zinc or magnesium doped calcium phosphates  
adding trifluoroacetic acid or metal carboxylates into the fuel.**

**Nanoparticle morphology**

**At a molar ratio of Ca/P < 1.5 promoted the formation of dicalcium pyrophosphate  
( $\text{Ca}_2\text{P}_2\text{O}_7$ ).**

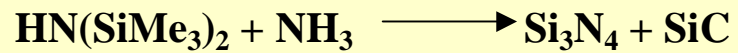
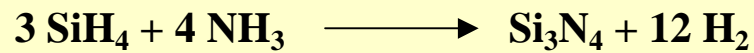
**Phase pure tricalcium phosphate TCP -  $\text{Ca}_3(\text{PO}_4)_2$   
obtained with a precursor Ca/P ratio of 1.52 after subsequent calcination at 900 °C**

**micropores and the facile substitution of both anions and cations  
possible application as a biomaterial.**

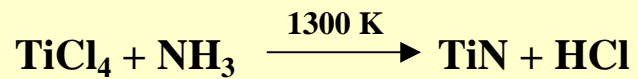


# Gas Phase Reactions

**High-power CO<sub>2</sub> lasers**



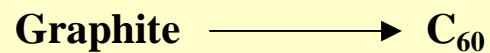
**DC-Ar Plasma**



**Tarnishing of Metal Surfaces**

**oxide, hydroxide layers**

**Arc**



# Vapor Phase Transport Syntheses

Sealed glass tube reactors

Solid reactant(s) A + gaseous transporting agent B

Temperature gradient furnace  $\Delta T \sim 50 \text{ }^\circ\text{C}$

Equilibrium established  $\text{A(s)} + \text{B(g)} \leftrightarrow \text{AB(g)}$

Equilibrium constant K

A + B react at  $T_2$

Gaseous transport by AB(g)

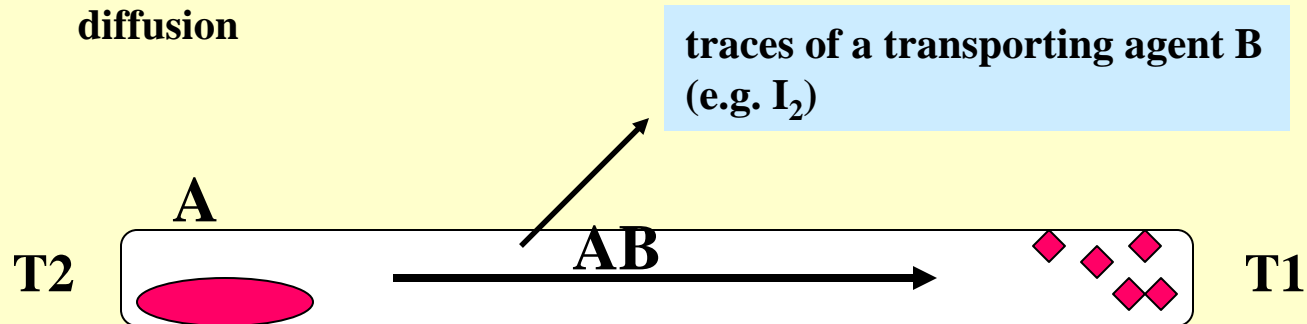
AB(g) decomposes back to A(s) at  $T_1$ , crystals of pure A

Temperature dependent K

Equilibrium concentration of AB(g) changes with T

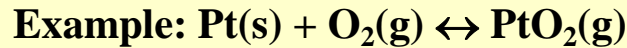
Different at  $T_2$  and  $T_1$

Concentration gradient of AB(g) = driving force for gaseous diffusion



# Vapor Phase Transport Syntheses

Whether  $T_1 < T_2$  or  $T_1 > T_2$  depends on the thermochemical balance of the reaction !  
Transport can proceed from higher to lower or from lower to higher temperature



**Endothermic reaction,  $\text{PtO}_2$  forms at hot end, diffuses to cool end, deposits well formed Pt crystals, observed in furnaces containing Pt heating elements**

**Chemical vapor transport,  $T_2 > T_1$ , provides concentration gradient and thermodynamic driving force for gaseous diffusion of vapor phase transport agent  $\text{AB(g)}$**

## **Uses of VPT**

- **synthesis of new solid state materials**
- **growth of single crystals**
- **purification of solids**

# Vapor Phase Transport Syntheses

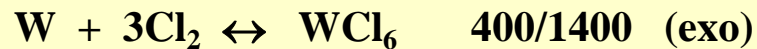
## Thermodynamics of VPT

Reversible equilibrium needed:  $\Delta G^\circ = -RT \ln K_{\text{equ}} = \Delta H^\circ - T\Delta S^\circ$

✎ Exothermic  $\Delta H^\circ < 0$

Smaller T implies larger  $K_{\text{equ}}$

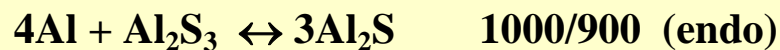
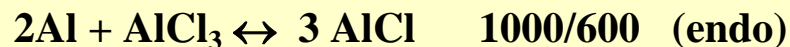
AB forms at cooler end, decomposes at hotter end of reactor



✎ Endothermic  $\Delta H^\circ > 0$

Larger T implies larger  $K_{\text{equ}}$

AB forms at hotter end, decomposes at cooler end of reactor



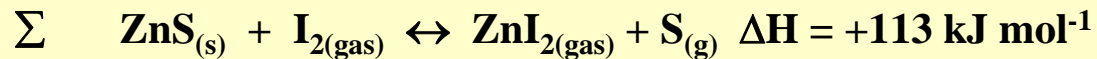
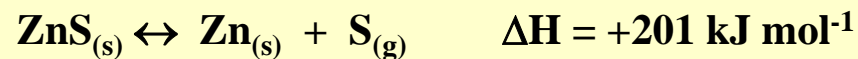
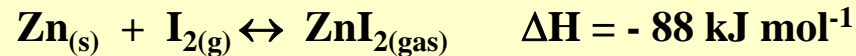
van't Hoff equation

$$\ln K_2 - \ln K_1 = \ln \frac{K_2}{K_1} = \frac{\Delta H^\circ}{R} \left( \frac{1}{T_1} - \frac{1}{T_2} \right)$$

# Vapor Phase Transport Syntheses

Estimation of the thermochemical balance ( $\Delta H$ ) of a transport reaction:

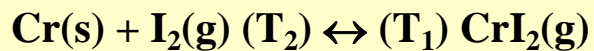
e.g.:



endothermic reaction, transport from hot to cold!

## Applications of VPT Methods

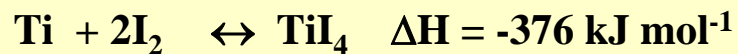
### ●\* Purification of Metals: Van Arkel Method



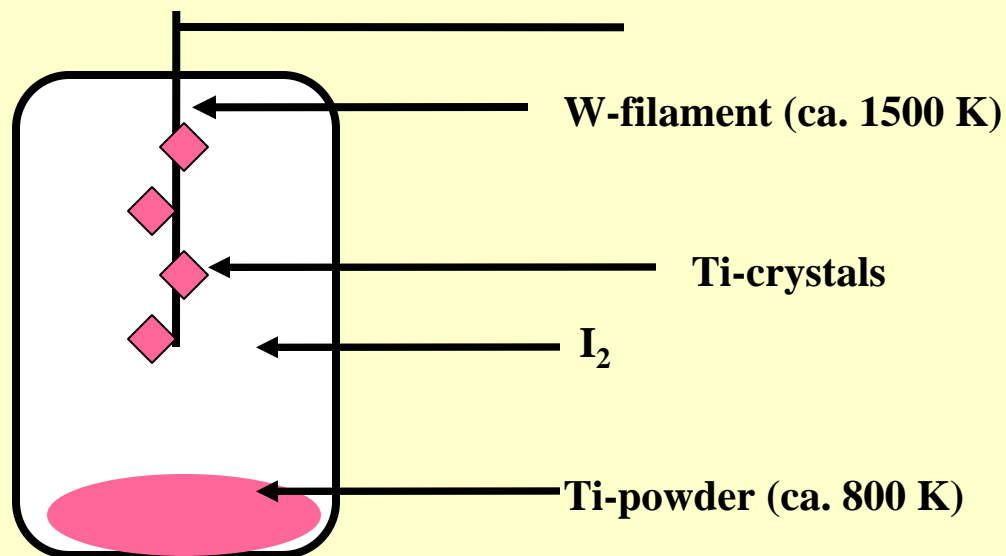
Exothermic,  $\text{CrI}_2(\text{g})$  forms at  $\text{T}_1$ , pure  $\text{Cr(s)}$  deposited at  $\text{T}_2$

Useful for Ti, Hf, V, Nb, Cu, Ta, Fe, Th

Removes metals from carbide, nitride, oxide impurities



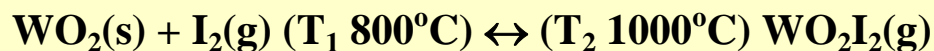
exothermic: transport from cold to hot



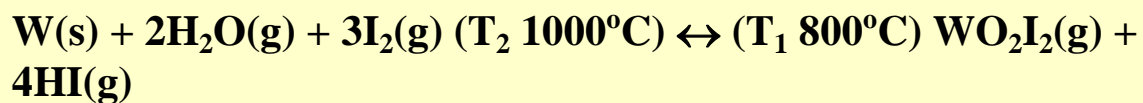
## Applications of VPT Methods

### ●\* Double Transport Involving Opposing Exothermic-Endothermic Reactions

**Endothermic:**



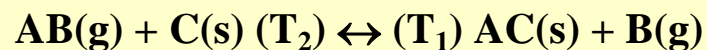
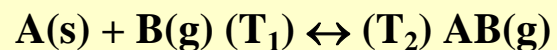
**Exothermic:**



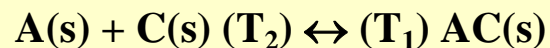
The antithetical nature of these two reactions allows W/WO<sub>2</sub> mixtures to be separated at different ends of the gradient reactor using H<sub>2</sub>O/I<sub>2</sub> as the transporting VP reagents

## Applications of VPT Methods

### ☛ Vapor Phase Transport for Synthesis

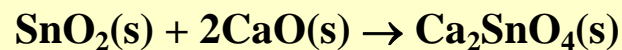


**Concept:** couple VPT with subsequent reaction to give overall reaction:

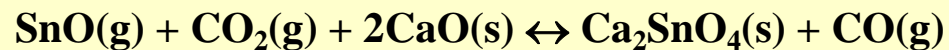
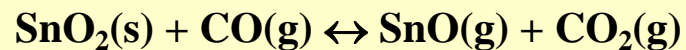


**Examples:**

**Direct reaction sluggish even at high T**



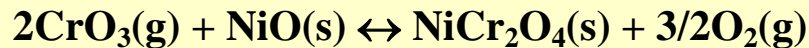
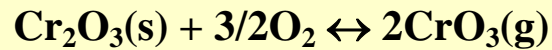
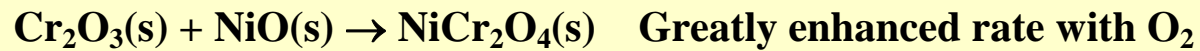
**Useful phosphor, greatly speeded up with CO as VPT agent:**



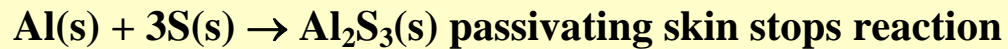


## Applications of VPT Methods

### Direct Reaction:

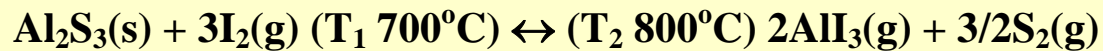


### Overcoming Passivation Through VPT



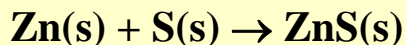
### In presence of cleansing VPT agent I<sub>2</sub>:

#### Endothermic:



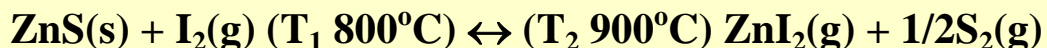
## **Applications of VPT Methods**

### **☛ Vapor Phase Transport for Synthesis**



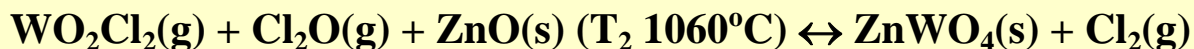
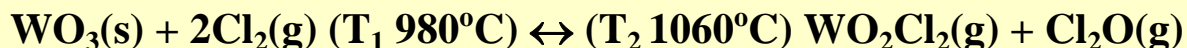
**passivation prevents reaction to completion**

**Endothermic:**

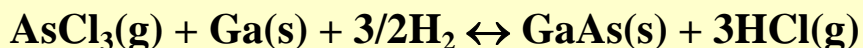


**VPT Synthesis of ZnWO<sub>4</sub>:**

**A Real Phosphor Host Crystal for Ag<sup>+</sup>, Cu<sup>+</sup>, Mn<sup>2+</sup>**

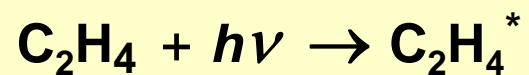


**Growing Epitaxial GaAs Films by VPT Using Convenient Starting Materials**



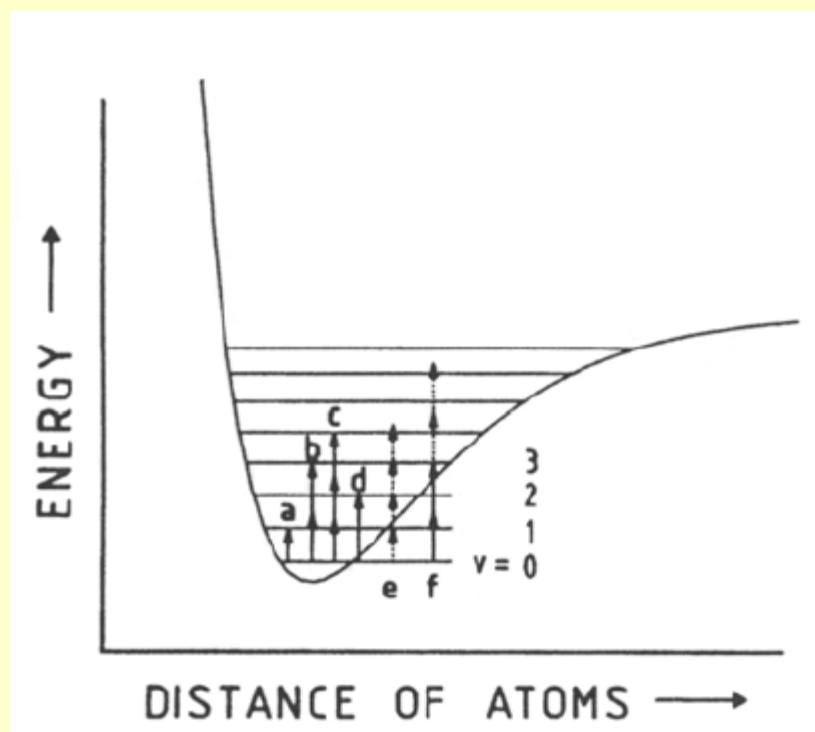
**Serves to establish initial equilibrium**

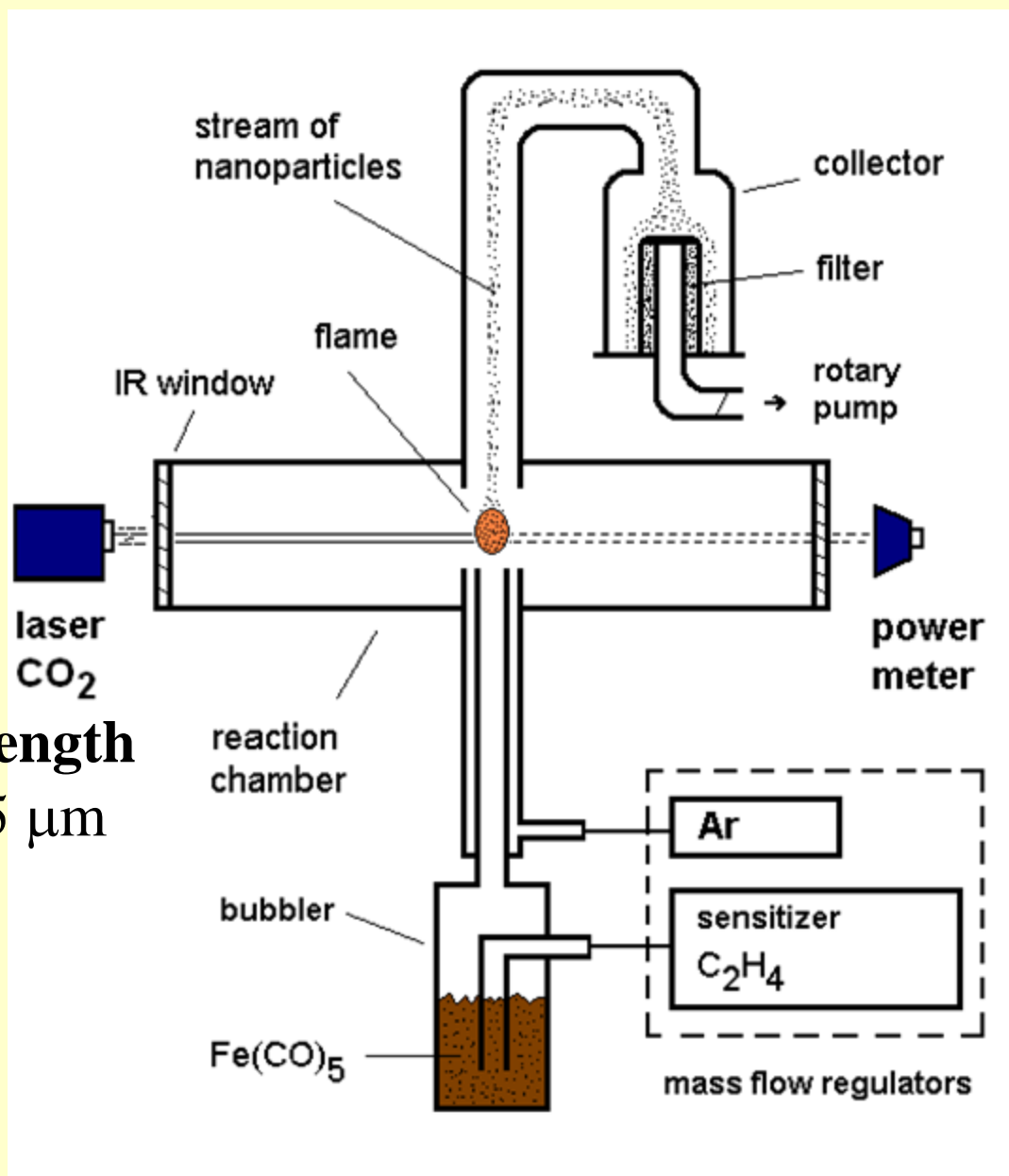
# Laser-induced homogeneous pyrolysis, LIHP



Excitation energy transferred to  
vibrational-translational modes

⇒ T increases





**laser wavelength**  
 $10.60 \pm 0.05 \mu\text{m}$

**Sensitizer**

SF<sub>6</sub>  
 $948 \text{ cm}^{-1}$

Isopropanol  
 $958 \text{ cm}^{-1}$

# Reaction Zone

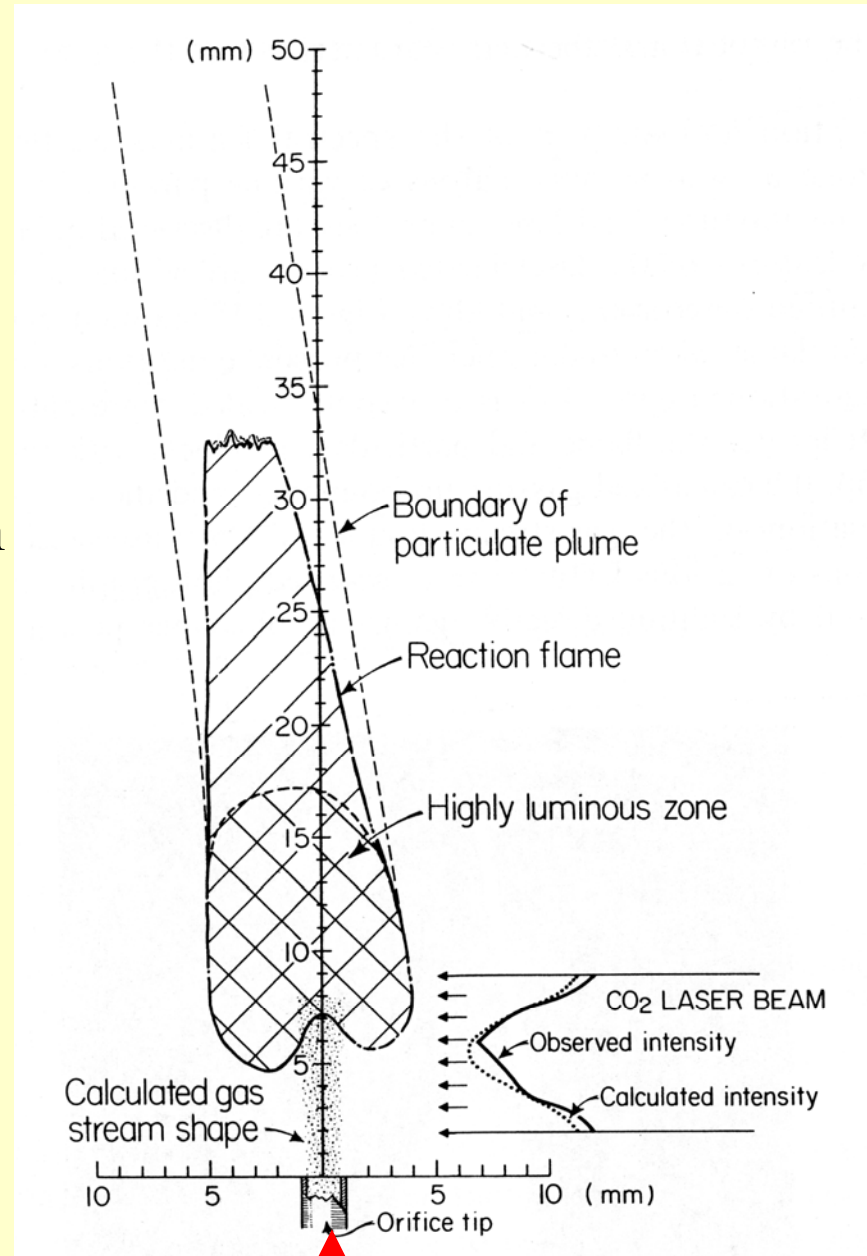
Overlap between  
the vertical reactant gas stream  
and the horizontal laser beam

away from the chamber walls

nucleation of nanoparticles

less contamination

narrow size distribution



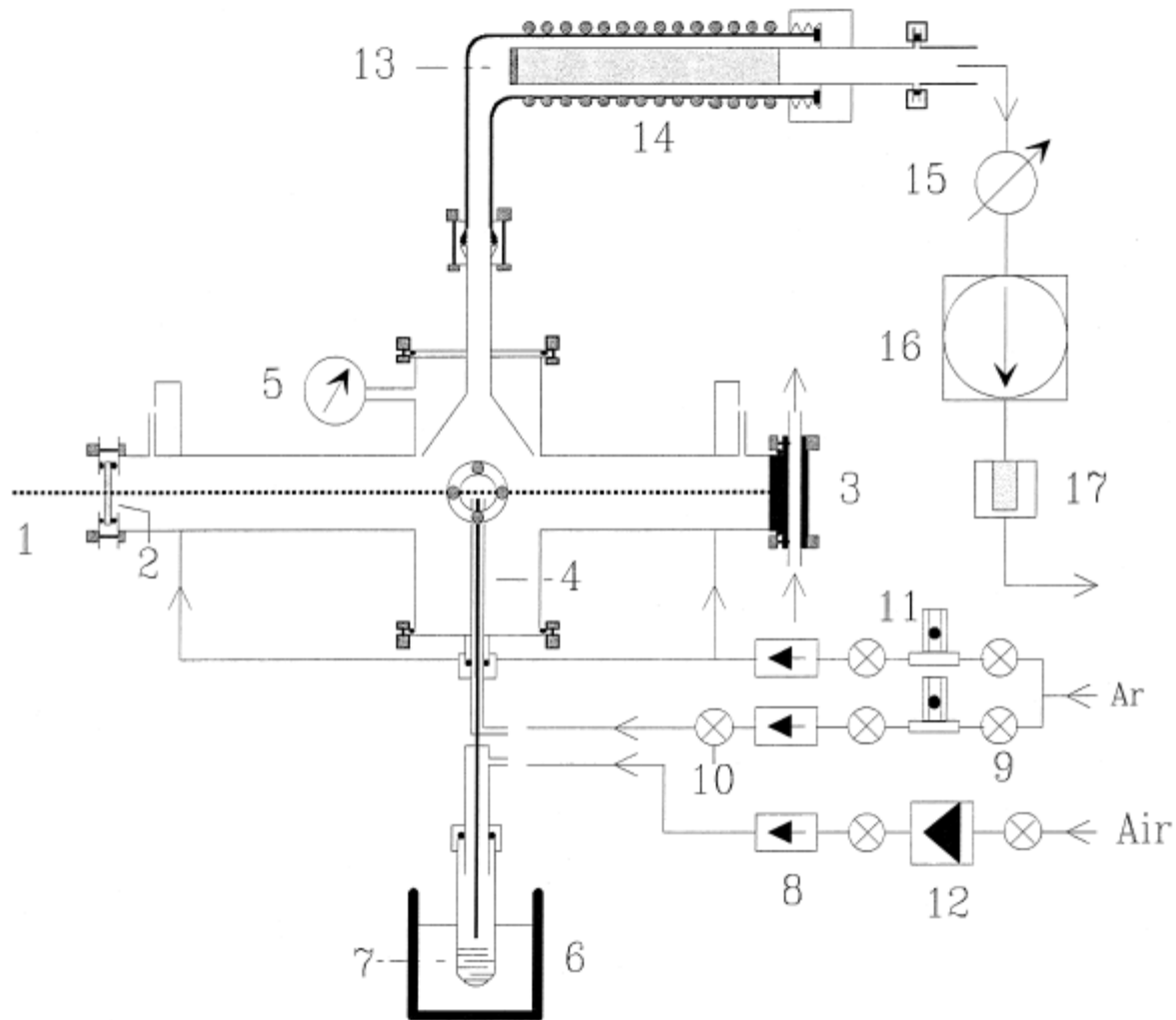
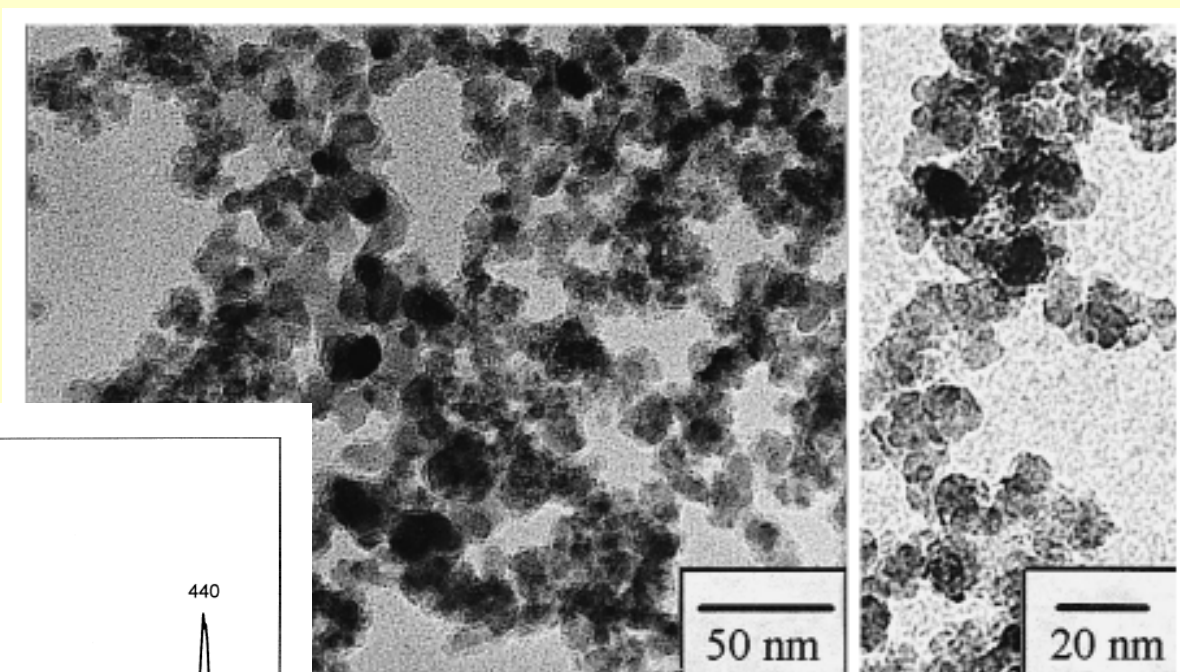
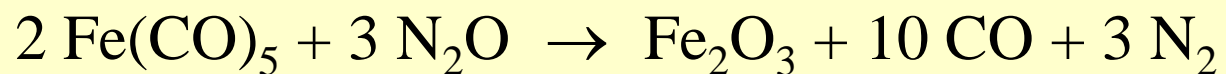


Fig. 1. CO<sub>2</sub> laser pyrolysis system. (1) Laser beam, (2) ZnSe window, (3) water refrigerated aluminium target, (4) nozzle, (5) pressure gauge, (6) ultrasonic bath, (7) 30% iron pentacarbonyl solution in isopropanol, (8) not return valve, (9) ball valve, (10) three ways ball valve, (11) argon rotameter, (12) massic controller of air flux, (13) stainless steel filter to collect the produced powders, (14) heating resistance, (15) pressure controller valve, (16) rotary vacuum pump, (17) filter to capture oil mist.

# Iron-oxide Nanoparticles by Laser-induced Pyrolysis



TEM micrographs of the synthesised  $\gamma\text{-Fe}_2\text{O}_3$  particles.

